IMPROVED HYDRODYNAMIC EFFICIENCY OF PONTOON -TYPE FLOATING BREAKWATERS

THEOHARRIS KOFTIS [1] and PANAYOTIS PRINOS [2]

[1]PhD candidate, Hydraulics Lab., Dept. of Civil Engineering,
Aristotle University of Thessaloniki, 54124, Greece
(Tel: +30-2310-995877, e-mail: thkoftis@civil.auth.gr)
[2]Professor, Hydraulics Lab., Dept. of Civil Engineering,
Aristotle University of Thessaloniki, 54124, Greece
(Tel: +30-2310-995689, Fax: +30-2310-995672, e-mail: prinosp@civil.auth.gr)

Abstract

The efficiency of a pontoon-type fixed floating breakwater (FB) is investigated numerically with the use of the COBRAS model. The RANS equations, combined with a k-ε turbulence model, and the VOF technique for tracking the free surface are used in a 2D vertical plane. The study is focused on the effects of the FB shape on the hydrodynamic characteristics of the structure (wave overtopping, transmission and reflection characteristics and flow velocity and turbulence). The studied FB configurations are a rectangular, and a trapezoid with slope of 45o, under the action of monochromatic waves. Surface elevation, RTD coefficients and detailed velocities and turbulence kinetic energy around the structure are presented. The efficiency of the FB, acting mostly in a reflective manner, is improved considerably when the shape is trapezoid and wave overtopping occurs, due to higher energy dissipation around the structure.

Keywords: Wave-structure interaction; Floating breakwater; RANS equations; Hydrodynamics; Turbulence

1. INTRODUCTION

Floating breakwaters (FBs) are among the environmentally friendly coastal structures which may be used for wave protection and restoration of semi-protected coastal regions with generally mild wave conditions. The study of FBs has been the focus of many coastal and ocean engineers for many years. Bruce and McCartney (1985) categorized the various floating breakwaters types, depending on the materials and type of construction, their limitations, and some design considerations. Isaacson (1993) gave the general guidelines for the design process for FBs and the related design criteria with respect to wave effects.

Several mathematical models have been developed for the investigation of the flow around a FB. Isaacson (1982) applied a numerical model based on potential theory coupled with the equations of motion for the rigid body, to obtain the flow characteristics and the dynamic response of a floating body. An application of the model was presented for the cases of a solitary wave and a linear intermediate to shallow water wave acting on a fixed surface-

piercing vertical circular cylinder. Williams (1997) and Williams et al (2000) also, applied linear potential theory and used the boundary integral equation method with an appropriate Green's function to obtain the hydrodynamic properties of a pair of floating pontoon breakwaters. The results presented for dimensionless wavenumber $kD < 4$ covering the range from shallow to deep water waves and gave a strong dependence of the reflection on width (W), draught (dr) and spacing of the pontoon. Koutandos et al (2004) investigated the wave-FB interaction numerically, with the use of Boussinesq equations combined with a potential theory model under the breakwater area. Chen et al (2004) presented a Dual Boundary Element Method (DBEM) for the study of a thin (zero thickness) submerged breakwater, and the relation of the transmission and reflection coefficients to the height and inclination angle of the structure.

The purpose of this study is to investigate numerically the effects of the structure shape on the hydrodynamic characteristics, including wave overtopping. Such a study requires a detailed analysis of the flow near and over the FB, such as 2DV velocity field, turbulence effects, which have not been found in previous numerical studies. The model is based on the 2D-V Reynolds Averaged Navier-Stokes (RANS) equations which are the most appropriate for studies of wave-structure interaction. In this study, the COBRAS (COrnell Breaking Waves and Structures) model, developed by Liu and Lin (1997), is used. The model considers wave reflection, transmission, overtopping and breaking due to waves, and 2DV hydrodynamics properties of the flow near the FB

2. NUMERICAL MODEL

The model solves the 2D-V Reynolds Averaged Navier-Stokes (RANS) equations in conjunction with transport equations for k and ε for the calculation of the Reynolds stresses. The model uses the Volume of Fluid (VOF) method (Hirt and Nichols (1981) to "track" the free surface location and the partial cell treatment in order to represent solid objects of arbitrary shape. Details can be found in Liu and Lin (1997). A brief summary of the boundary, initial conditions and solution procedure used in the COBRAS model is presented in the following paragraphs.

2.1 BOUNDARY AND INITIAL CONDITIONS

The boundary conditions for the mean and turbulence quantities are summarized in the following paragraph. The dynamic free surface boundary condition is applied for the mean flow velocities, which is equivalent to the zero stress free surface condition if no stresses are applied on the free surface. For the k and ε the zero normal gradient boundary condition is applied at the free surface, indicating that turbulence does not diffuse across the free surface. At the rigid boundaries (bed and FB walls) the no-slip condition is applied and the "wall function" approach is implemented at the first near-wall grid point. This avoids a refined modeling of the viscous sub-layer which would be computationally expensive. Also a low level of turbulent kinetic energy k is assumed as initial condition in order to maintain stability

(Lin and Liu 1998). Radiation boundary conditions are set at both sides of the computational domain to allow outgoing waves.

Additionally a sponge layer- an additional exponential damping function term added to the original momentum - is imposed at the left boundary, next to the source function, in order to fully absorb the waves that propagate in the opposite direction of the zone of interest.

2.2 WAVE GENERATION

The waves are generated by the source function method (Lin and Liu 1999) in a rectangular source at a certain distance from the left side of the domain. The method consists of introducing a pressure variation within the source region cells, in order to generate various types of waves. In this study monochromatic waves have been generated.

2.3 FREE SURFACE TRACKING METHOD

The VOF method (Hirt and Nichols, 1981) is used for "tracking" the free surface variation. The donor-acceptor method is used for the free surface reconstruction. The partial cell treatment is used for representing solid objects of arbitrary shape.

2.4 SOLUTION PROCEDURE

The solution of the RANS equations is based on the two-step projection method (Chorin 1968) with the use of the finite difference method. The convection terms in the momentum equations are discretized by a combination of the upwind and central difference scheme in order to produce stable and accurate results. The central difference method is used to express the stress gradient and the pressure gradient and the forward time-differencing method for the time derivatives. Similar expressions are used for the k-ε transport equations.

3. NUMERICAL IMPLEMENTATION-ANALYSIS OF RESULTS

A numerical wave tank shown in Fig. 1, with dimensions 60m x 2.5 m is used. The incident monochromatic waves with wave height H = 0.25 m and wave period T=2.04 sec and 3.16 sec, are generated at a distance of 1.5 L from the left side of the domain. Several grids have been employed to test the grid dependency of the results. It is found that the same results are obtained for the water surface elevation and the velocity field even if a coarser grid is used. This is not the case for the turbulent quantities for which the grid dependency is stronger. Finally a variable mesh, which is finer close to the FB, is installed for more accurate of the turbulent quantities, with 4 sub-meshes in the x-direction, with $0.04<\Delta x<0.02$ and 2 sub-meshes in the y-direction, with $0.02<\Delta y<0.01$. The computational time-step, restricted by the CFL criterion, takes a maximum value of 0.005 sec, leading to time consuming numerical tests. The total computational time for these tests was taken 20T, and the results presented are from 15-20 T.

The FB examined in this study has a width W=2.0m and a height H_{br}=0.90 m, which correspond to the common used dimensions in prototype scale (W=4.0m, H_{br}=1.80 m) with

a scale parameter of 0.5. The examined shapes are a rectangular, and a trapezoid with slope of 45o, both with draught dr =0.65 m, (Fig. 2) against waves with T= 2.04 and 3.16 sec. The dimensions of the wave tank and the FB are those of available large scale experiments (Koutandos et al, 2004). The numerical model is validated against experimental data for the rectangular FB and then it is applied to the trapezoid FB case. Finally, the hydrodynamic properties of the flow in the vicinity of the FB are described in detail for both cases.

3.1 ANALYSIS OF RESULTS

Transmission, reflection and dissipation coefficients (CT, CR, and CD respectively), for the two FB configurations together with the experimental results (Koutandos et al, 2005) for the case of the rectangular FB are shown in Table 1.

Table 1. Numerical and Experimental CT,CR ,CD coefficients

	Rectangular T=2.04 s	Exp. Data T=2.04 s	Trapezoid T=2.04 s	Rectangular T=3.16 s	Exp. Data T=3.16 s	Trapezoid T=3.16 s
CT	0.21	0.25	0.11	0.53	0.60	0.38
CR	0.85	0.88	0.78	0.67	0.62	0.52
CD	0.48	0.41	0.62	0.52	0.51	0.76

It is shown that the performance of the FB is highly reduced for longer waves and that the FB acts generally in a reflective manner. For the case of the trapezoid FB better results are obtained since the transmission coefficient is reduced by about 50% for T= 2.04 sec and 30% for T= 3.16 sec. For both FB configurations the reflection is similar, while reduced transmission and increased dissipation are found for the trapezoid FB. This shows the greater energy dissipation that occurs in the sloping face of the FB, which is responsible for the reduced transmitted waves. This can be seen also from Fig. 3 where the envelopes of the reflective and transmitted waves are shown. The same partial standing wave for both FB configurations is shown together with the reduced transmitted waves for the trapezoid FB, showing the dissipative manner of such a structure. Also, a small amount of wave overtopping occurs for the trapezoid FB and mainly for the shorter wave, which results in a transmitted wave composed of waves passing underneath and over the structure with a phase depending on the breakwater width (W). The influence of the wave overtopping on transmission is not clear and a detailed study should be conducted on the dimensions of a FB.

The dissipation, observed in the trapezoid FB, can be seen from the detailed hydrodynamic properties of the flow in the vicinity of the FB. In Figs. 4-5 the mean velocity field is shown for both FBs, while Figs. 6-7 show the turbulent kinetic energy field, for waves with T=3.16 sec.

The flow pattern of the rectangular FB is shown in Fig. 4, where the phase t/T=18.0 corresponds to the maximum value of the wave crest in the seaward side. The velocities are

higher in the seaward corner of the FB and in general twice higher than those in the leeward side for all the phases. The velocity takes a maximum value of 1.154 m/sec at t/T=18.50 in the seaward side with direction upwards. For the trapezoid FB the flow pattern is much more intense. For t/T=18.0 a much bigger eddy is formed in the seaward side, caused by the complicated flow conditions, with the return flow on the sloping face interacting with the up going fluid. Also in the leeside considerable velocities occur and two counter rotating vortices can be seen. The flow field in the next phase continues with the velocity vectors in the seaside have directions toward the bottom of the FB, taking maximum values of 1.4 m/sec.

The pattern of the turbulent kinetic energy field is shown in Fig. 5 (line increment is 0.01 m2/sec2). Maximum value of k= 0.05 m2/sec2 occurs in the seaward side at t/T=18.0, and very small values are observed in the lee side of the FB. The corresponding turbulent kinetic energy field reflects the much more complicated flow field for the trapezoid FB. As can be seen from the contours of k for the trapezoid FB, turbulence is spread in a much larger area and with about three times the values as compared with that of the rectangular FB. The maximum value of k=0.16 m2/sec2 occurs at t/T=18.75 in the seaside of the FB. Also the trajectory of maximum values of k follows that of the formed eddies as in the rectangular FB.

4. CONCLUSIONS

A new shape for a pontoon-type floating breakwater with improved hydrodynamic characteristics has been studied numerically with the use of the COBRAS model. The trapezoid FB tested against two wave conditions and in both cases the results showed an overall improvement in comparison with a typical rectangular one. The trapezoid FB shows reduced wave transmission and increased energy dissipation in its inclined front face for the conditions examined.

ACKNOWLEDGEMENTS

The authors acknowledge the financial support of the General Secretariat for Research and Technology (G.S.R.T.) through the program “Environmental Coastal Management with the use of Floating Breakwaters.

REFERENCES

Bruce, L., McCartney, M. (1985). “Floating breakwater design”, Journal of Waterway, Port, Coastal and Ocean Engineering, Vol. 111(2), pp. 304-318.

Chen, K.-H., Chen, J.-T., Lin, S.-Y. and Lee, Y. T. (2004). “Dual Boundary Element Analysis of Normal Incident Wave Passing a Thin Submerged Breakwater with Rigid, Absorbing, and Permeable Boundaries”, Journal of Waterway, Port, Coastal and Ocean Engineering, Vol. 130(4), pp. 179-191.

Chorin, A.J. (1968). “Numerical solution of the Navier-Stokes equations”, Mathematics of Computation, Vol. 22, pp. 745-762.

Hirt, C.W., Nichols, B.D. (1981). “Volume of Fluid (VOF) Method for the Dynamics of Free Boundaries”, Journal of Computational Physics, Vol. 39, pp. 201-225.

Isaacson, M. (1982). "Nonlinear-wave effects on fixed and floating bodies", Journal of Fluid Mechanics, Vol. 120, pp. 267-281.

Isaacson, M. (1993). "Wave Effects on Floating Breakwaters", Proceedings of Canadian Coastal Conference 1993, Vancouver, Canada, pp. 53-65.

Koutandos, E. V., Karambas Th. V. and Koutitas C. G. (2004). "Floating Breakwater Response to Waves Action Using a Boussinesq Model Coupled with a 2DV Elliptic Solver", Journal of Waterway, Port, Coastal and Ocean Engineering, Vol. 130(5), pp. 243-255.

Koutandos, E., Prinos, P., Gironella, X. (2005). "Floating breakwaters under regular and irregular wave forcing- Reflection and transmission characteristics", Journal of Hydraulic Research, Vol. 43, No.2, pp. 174-188.

Lin, P., Liu, L.-F. P. (1998). "A numerical study of breaking waves in the surf zone", Journal of Fluid Mechanics, Vol. 359, pp. 239-264.

Lin, P., Liu, L.-F. P. (1999). "Internal wave-maker for Navier-Stokes equation models", Journal of Waterway, Port, Coastal and Ocean Engineering, Vol. 125(4), pp. 207-215.

Liu, L.-F. P., Lin, P. (1997). A numerical model for breaking waves: The Volume of Fluid Method, Research Report. No. CACR-97-02, Center for Applied Coastal Research, Ocean Engineering Laboratory, University of Delaware.

Williams, A.N., Abul-Azm, A.G. (1997). "Dual pontoon floating breakwater", Ocean Engineering, Vol. 24, pp. 465-478.

Williams, A.N., Lee, H.S., Huang, Z. (2000). "Floating pontoon breakwater", Ocean Engineering, Vol. 27, pp. 221-240.

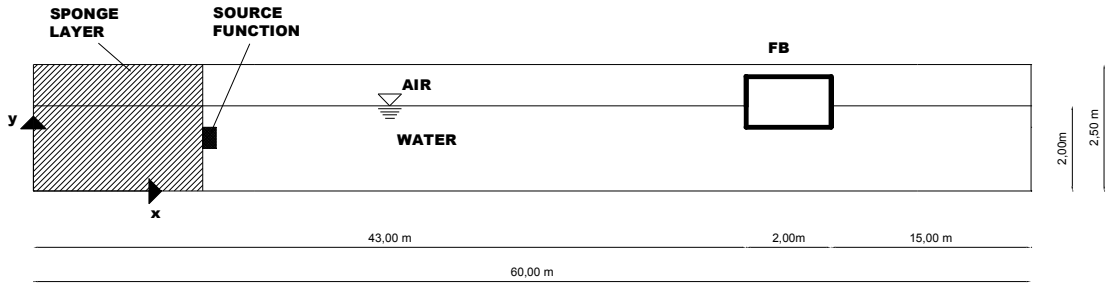

Fig.1 Numerical wave tank and floating breakwater.

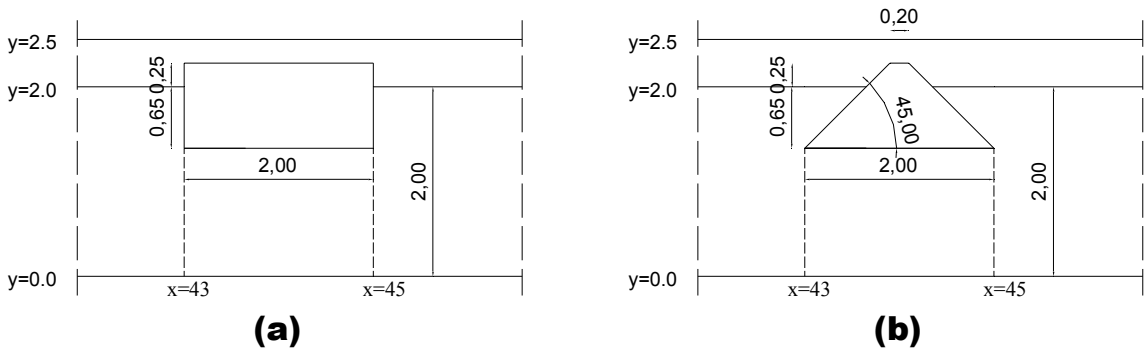

Fig. 2 Floating Breakwater configurations: (a) Rectangular breakwater, (b) Trapezoid breakwater with slope 45o

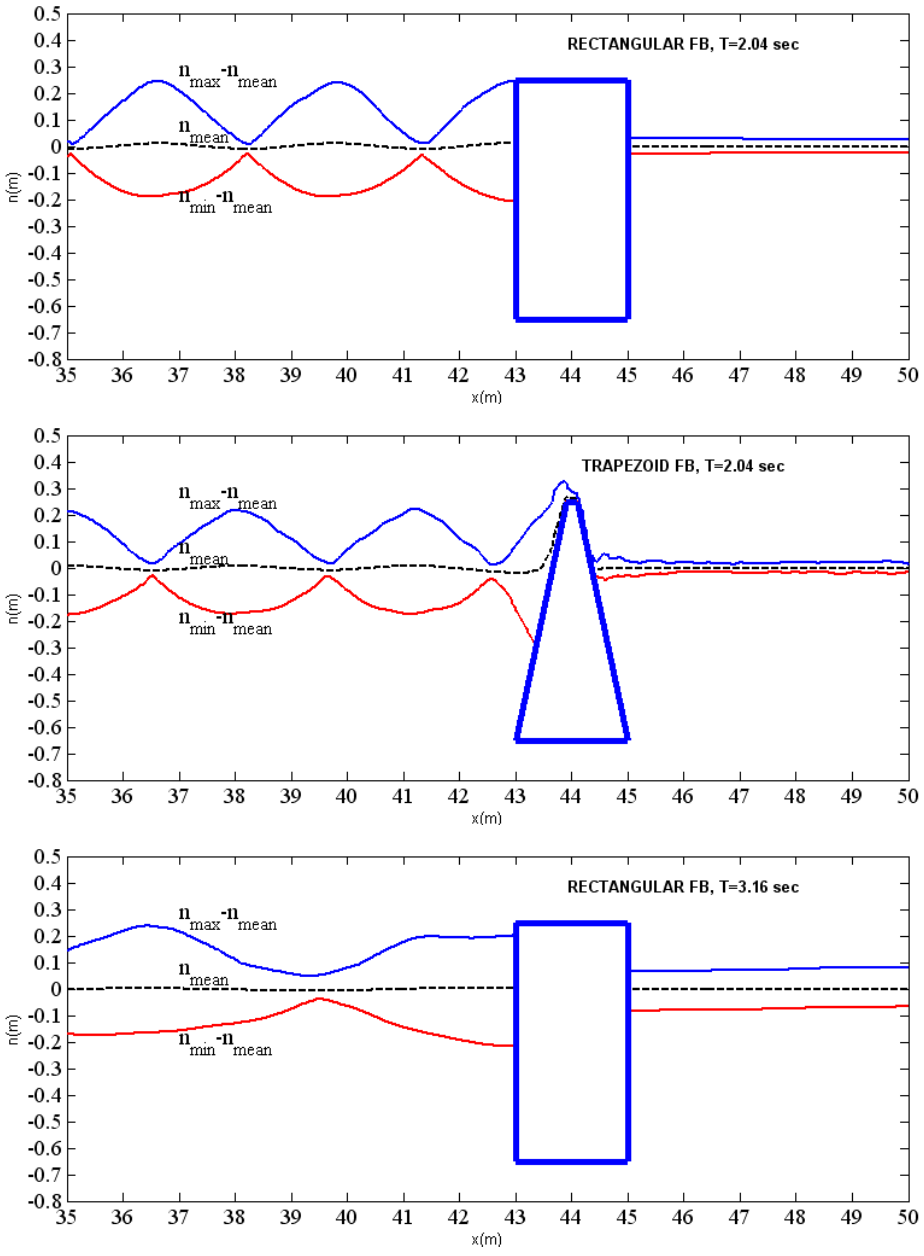

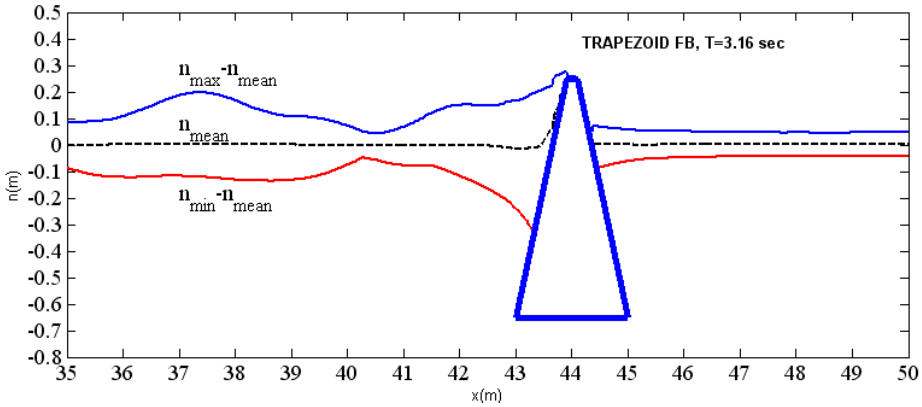

Fig. 3 Wave height envelopes and mean water level for the two FB configuration and incident wave periods.

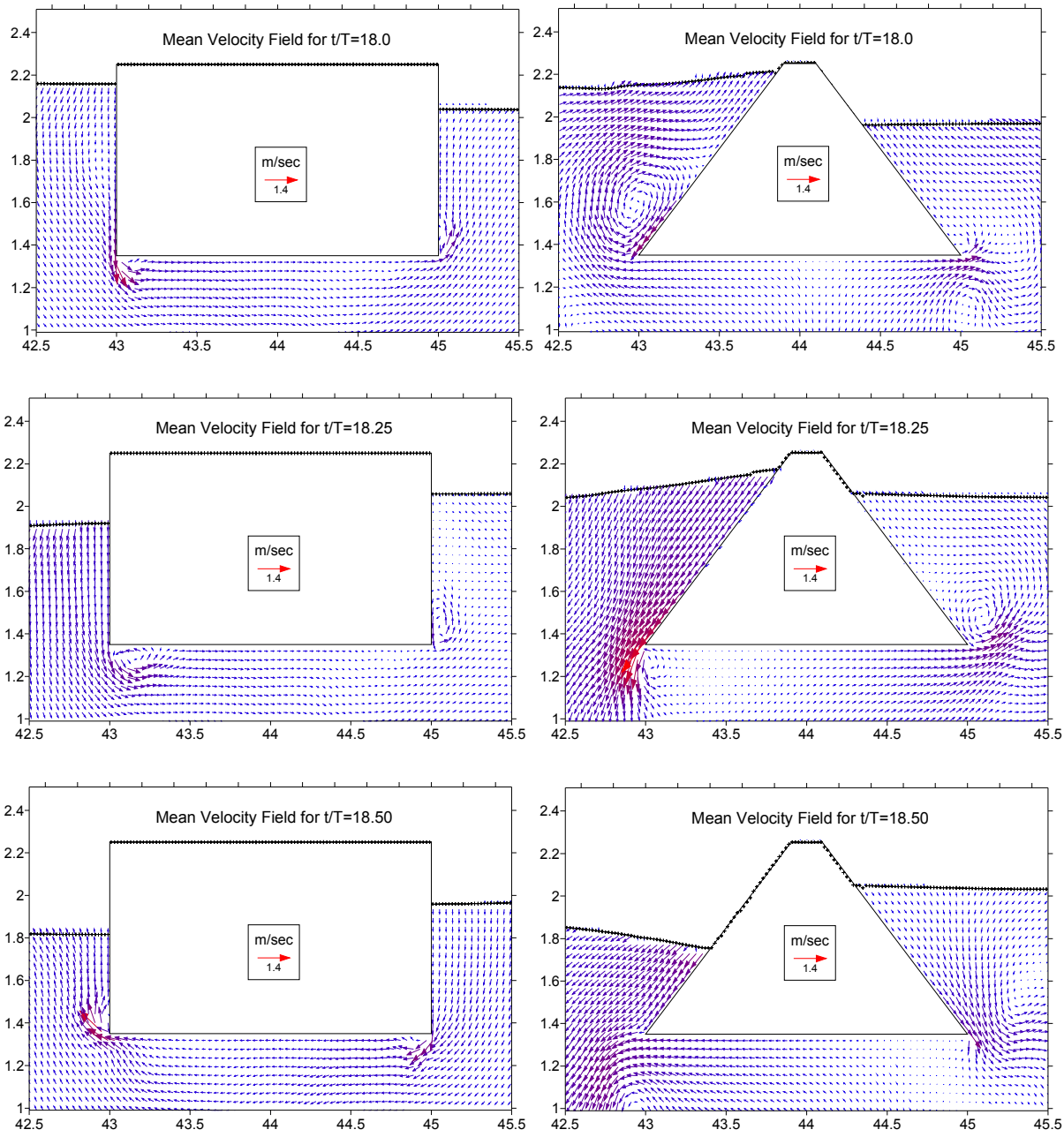

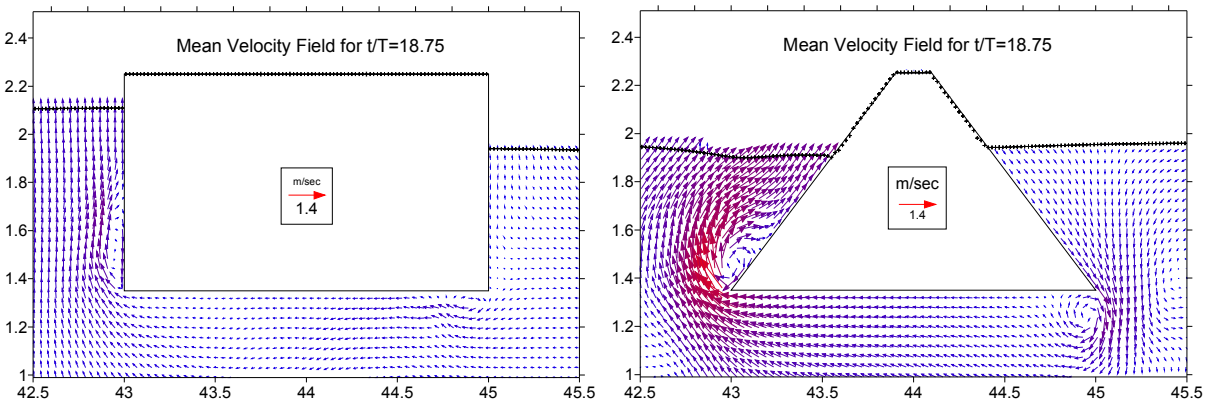

Fig. 4Mean velocity field in a wave cycle (T=3.16sec)

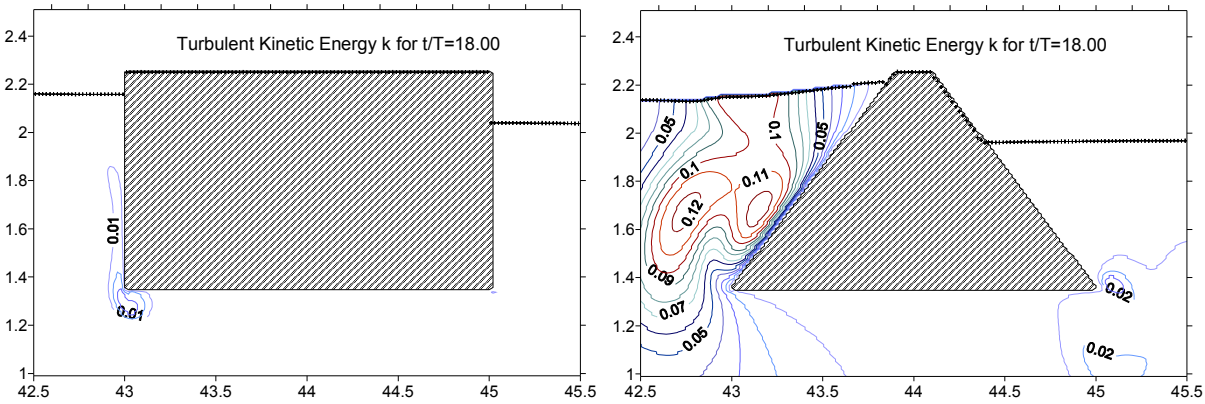

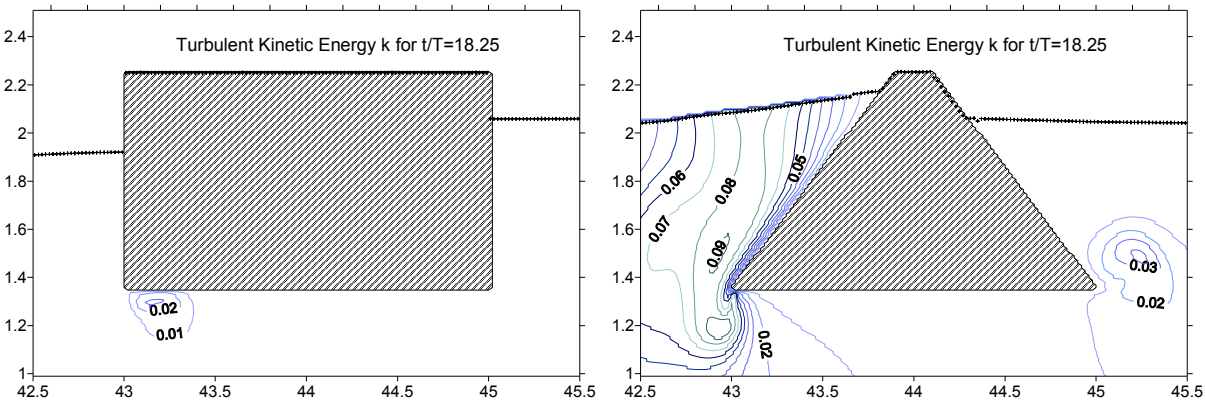

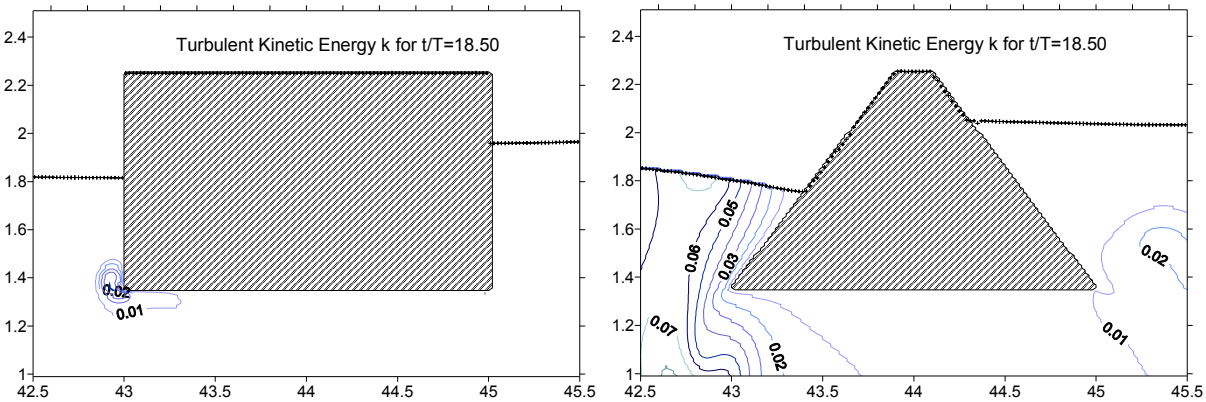

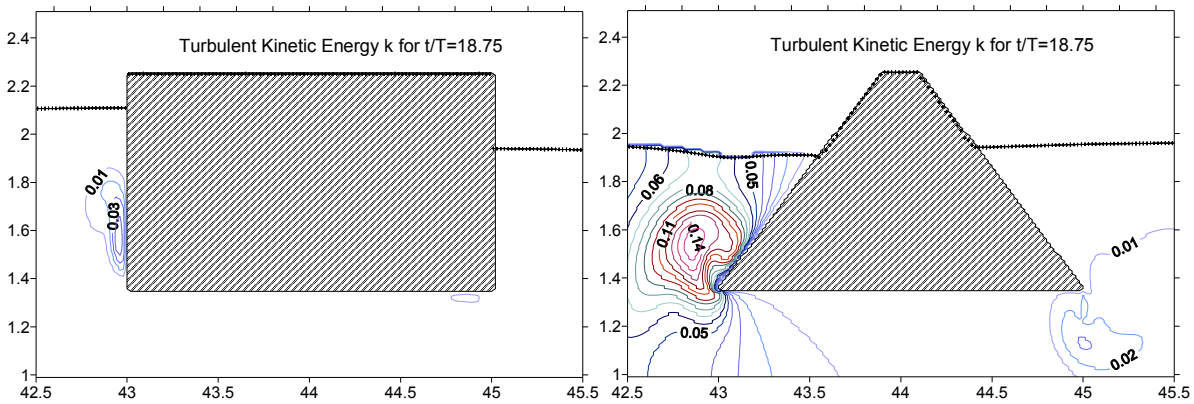

Fig. 5 Turbulent kinetic energy field in a wave cycle (T=3.16sec)